Accepted Manuscript

Adhesion and collisional release of particles in dense planetary rings

Anna Bodrova, Jürgen Schmidt, Frank Spahn, Nikolay Brilliantov
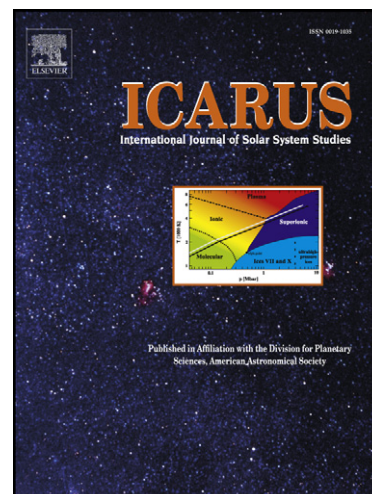
Please cite this article as: Bodrova, A., Schmidt, J., Spahn, F., Brilliantov, N., Adhesion and collisional release of particles in dense planetary rings, *Icarus* (2011), doi: 10.1016/j.icarus.2011.11.011

Adhesion and collisional release of particles in dense planetary rings

Anna Bodrova[a,b], Jürgen Schmidt[a], Frank Spahn[a], Nikolay Brilliantov[c]

[a]*Institute of Physics and Astronomy, University of Potsdam, 14476, Potsdam, Germany*
[b]*Department of Physics, Moscow State University, Leninskie Gory, 119991, Moscow, Russia*
[c]*Department of Mathematics, University of Leicester, Leicester LE1 7RH, United Kingdom*

Abstract

We propose a simple theoretical model for aggregative and fragmentative collisions in Saturn's dense rings. In this model the ring matter consists of a bimodal size distribution: large (meter sized) boulders and a population of smaller particles (tens of centimetres down to dust). The small particles can adhesively stick to the boulders and can be released as debris in binary collisions of their carriers. To quantify the adhesion force we use the JKR theory (Johnson, Kendall and Roberts, 1971). The rates of release and adsorption of particles are calculated, depending on material parameters, sizes, and plausible velocity dispersions of carriers and debris particles. In steady state we obtain an expression for the amount of free debris relative to the fraction still attached to the carriers. In terms of this conceptually simple model a paucity of subcentimeter particles in Saturn's rings (French and Nicholson, 2000; Marouf et al., 2008) can be understood as a consequence of the increasing strength of adhesion (relative to inertial forces) for decreasing particle size. In this case particles smaller than a certain critical radius remain tightly attached to the surfaces of larger boulders, even when the

boulders collide at their typical speed. Furthermore, we find that already a mildly increased velocity dispersion of the carrier-particles may significantly enhance the fraction of free debris particles, in this way increasing the optical depth of the system.

Keywords: Planetary rings, Saturn, rings, Collisional physics

1. Introduction

Saturn's dense ring system consists of a large number of water ice particles, which, owing to frequent mutual dissipative collisions, flattened into a thin disk (Colwell et al., 2009; Cuzzi et al., 2009; Schmidt et al., 2009). Light scattering properties of the rings are consistent with a power-law size distribution $n(r) \sim r^{-\beta}$ with a slope near $\beta = 3$, ranging from centimetres to tens of meters, varying with the radial distance from the planet (French and Nicholson, 2000; Showalter and Nicholson, 1990; Zebker et al., 1985, see also Cuzzi et al. 2009; Schmidt et al. 2009). In particular, a lack of particles smaller than, roughly, 1 cm (French and Nicholson, 2000) is implied by comparison of the optical depth of the main rings at different wavelength (from microwaves to UV), and detailed photometry of the A ring (Dones et al., 1993). Such a size distribution may arise from a balance of aggregation between particles and fragmentative collisions of aggregates (Davis et al., 1984; Weidenschilling et al., 1984). The adhesive forces, leading to aggregation, are strongest for small particles (Chokshi et al., 1993). Although small debris should be steadily created in hypervelocity impacts of micrometeoroids on the rings (Cuzzi and Durisen, 1990; Durisen, 1984), it seems plausible that it is rapidly and permanently adsorbed on the surfaces of the larger particles,

2

which would explain the small contribution of this particle size to the optical depth of the rings. This scenario was qualitatively discussed by Dones et al. (1993), who estimated the critical radius for sticking using the adhesion model proposed by Chokshi et al. (1993).

In this paper we investigate this idea quantitatively in terms of a kinetic model with a bimodal distribution of particle sizes, for binary adhesive and dissipative particle collisions. We consider consistently the kinetics of coagulation and fragmentation of particles. The balance of fragmentation of particles and their gravitational aggregation, leading to the establishment of the power-law size distribution in Saturn's rings was studied by Longaretti (1989). A simple model for ballistic aggregation and fragmentation was introduced recently by Brilliantov et al. (2009), however, without specifying a detailed mechanism of fragmentation.

We discuss the possibility that an increased velocity dispersion of the carrier-particles may significantly enhance the fraction of free debris particles, in this way increasing the optical depth of the system. Such a process may be important to understand quantitatively the observed brightness variations in perturbed ring regions, like satellite resonances (Dones et al., 1993; Nicholson et al., 2008) and the lobes of the propellers (Spahn and Sremčević, 2000) observed in the A ring (Sremčević et al., 2007; Tiscareno et al., 2006).

The plan of the paper is as follows. In Section 2 we present the theoretical model, and calculate release and sticking rates of debris particles on the surfaces of carriers. The balance of these processes is analyzed in Section 3, establishing a steady distribution of free debris, depending on the parameters of the model. We discuss our results and their applications to Saturn's rings

3

in Section 4, and give our conclusions in Section 5.

2. Model

We consider a bimodal system consisting of identical large boulders (carriers) of radius R and smaller particles with a range of radii $r << R$ (Fig. 1). Due to adhesion small particles can attach to the surface of bigger ones. We assume that boulders and debris particles are indestructible, while the fragmentation of the aggregates formed by carriers and attached debris is possible. Thus the total number of small particles of size r per unit volume $N_d(r)$ is comprised of free debris with number density $n_v(r)$ and a population covering the surface of boulders with surface density $n_s(r)$. Then the mass conservation implies:

$$N_d(r) = n_v(r) + 4\pi R^2 n_s(r) N_c \,, \tag{1}$$

where N_c is the number density of carriers. We neglect the change of carrier size due to the attached debris particles.

The equilibrium number density of small particles $n_v(r)$ (debris) arises from the balance of their aggregation with boulders and detachment in collisions of carriers. The kinetic equation, describing these processes reads

$$\frac{dn_v(r)}{dt} = I_+(r) - I_-(r) \,, \tag{2}$$

where I_+ is debris production rate (the number density of debris of radius r, released per unit time in unit volume), I_- - their adsorption rate (the number density of smaller particles, adsorbed at the surface of carriers per unit time in unit volume). I_+ and I_- are calculated below. We neglect the interaction of debris particles with each other.

4
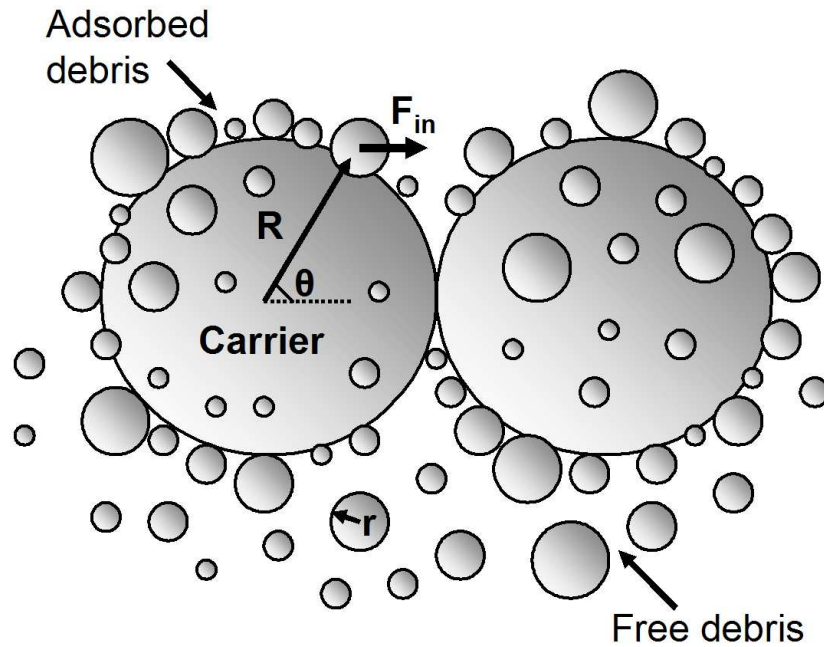
Figure 1: A bimodal system consisting of carriers of radius $R \sim 1$ m and debris of radii $r < 10$ cm. The debris can either move freely or be attached to the surface of carriers due to adhesive forces. Debris can be released during the collision of carriers, if the normal component of inertial force, acting on debris $F_{\text{in}} \cos \theta$ (Eq. 14) exceeds the adhesion force F_{sep} (Eq. 7). (Here θ is the angle between the line, connecting the centres of colliding carriers and the line, connecting the centres of the carrier and the debris particle, resting on its surface.) Debris particles can be re-adsorbed in subsequent collisions.

Let $\vec{V}_c$ and $\vec{V}_d$ be the velocities of carriers and debris particles measured in a frame that co-rotates with the local Keplerian speed at given distance from the central planet. We define the relative velocity of debris and carriers as $\vec{V}_{cd} = \vec{V}_c - \vec{V}_d$. Let us also denote the velocity dispersions of carriers and debris as $v_{c,d} = \sqrt{\langle V_{c,d}^2 \rangle}$.

Although the velocity distribution function of particles in Saturn's Rings is anisotropic (Goldreich and Tremaine, 1978), we do not expect a significant influence of this anisotropy on the average outcome of aggregation and fragmentation. For sake of simplicity we assume here an isotropic Maxwellian distribution of random (thermal) speeds of particles

$$f\left(\vec{V}_{c,d}\right) = \left(\frac{3}{2\pi v_{c,d}^2}\right)^{3/2} \exp\left(-\frac{3}{2}\frac{V_{c,d}^2}{v_{c,d}^2}\right) \tag{3}$$

For simplicity we assume, that the velocity dispersion v_d is equal for debris of all radii (Salo, 1992b). We also do not take into account the deviation of velocity distribution function from the Maxwellian (which corresponds to the Rayleigh distribution in orbit elements), found by Ohtsuki and Emori (2000) in the computer simulation of dense self-gravitating systems.

We assume, that all particles are composed of ice with Young modulus $Y = 7 \cdot 10^9$ Pa and Poisson ratio $\nu = 0.25$ (Chokshi et al., 1993). It is also common to introduce the elastic constant $D = \frac{3}{2}\frac{(1-\nu^2)}{Y} = 2 \cdot 10^{-10}\,\mathrm{Pa}^{-1}$. The material densities of carriers and smaller particles are also assumed to be equal: $\rho_c = \rho_d = 900\,\mathrm{kg/m}^3$.

The adhesive interactions are characterized by the adhesion coefficient γ, which is twice the surface tension coefficient. The adhesion coefficient was estimated theoretically for pure ice surfaces as $\gamma = 0.74\,\mathrm{N/m}$ (Chokshi

6

et al., 1993). Hatzes et al. (1991) have shown experimentally, that adhesive interactions of ice particles significantly depend on their surface structure. In the recent experiments of Gundlach et al. (2011) the adhesion coefficient of micrometer-sized ice particles was found to be $\gamma = 0.19\,\mathrm{N/m}$.

Adhesive interactions become important only in the final phase of a collision, while generally the impact phase is governed by elastic and dissipative forces. The latter tend to damp the relative motion. These dissipative losses are usually quantified by the restitution coefficient, defined as the ratio of the normal components of the relative velocity after and before an impact: $\varepsilon = \left| \left(\vec{V}_{cd}' \cdot \vec{e} \right) / \left(\vec{V}_{cd} \cdot \vec{e} \right) \right|$, where $\vec{V}_{cd}'$ is the relative velocity after the collision and $\vec{e}$ is a unit vector, along the line, joining centres of particles during their impact. In general, the restitution coefficient is velocity-dependent (Bridges et al., 1984; Brilliantov et al., 1996; Ramirez et al., 1999), but in the present study we assume it to be constant. We take here $\varepsilon \simeq 0.3$ as a typical value for the restitution coefficient for ice particles, colliding with relative velocities ~ 1 cm/s and effective radii ~ 1 cm (Bridges et al., 1984).

2.1. Debris adsorption rate

If $\vec{V}_{cd}$ is small enough, carriers and debris can form aggregates due to adhesion. The adhesive interaction can be described in the framework of JKR theory (Johnson, Kendall and Roberts, 1971).

The force, acting during the collision of a boulder with a smaller particle, consists of two parts (Johnson et al., 1971):

$$F_a = \frac{a^3}{DR_{cd}} - \sqrt{\frac{6\pi\gamma}{D}} a^{3/2} \tag{4}$$

The first term corresponds to the Herzian elastic force, the second one -

7
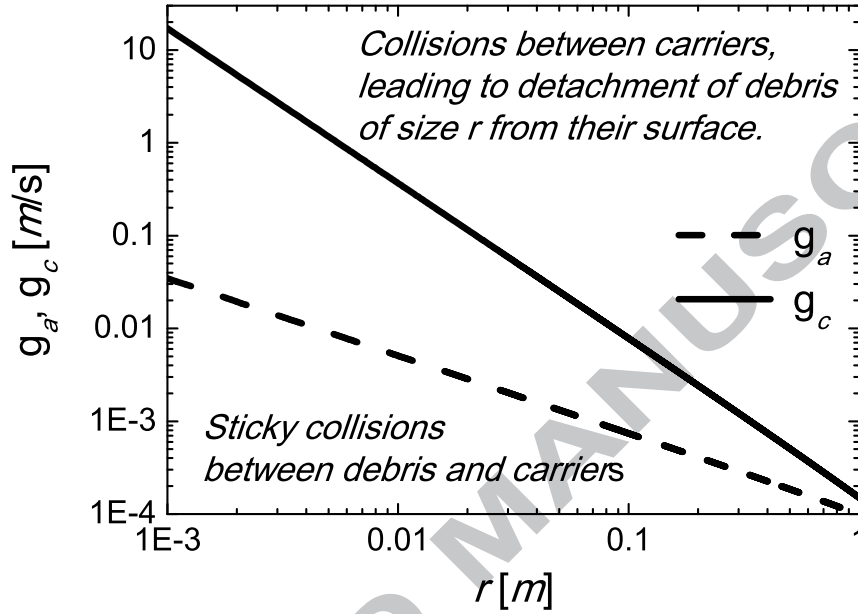
Figure 2: Maximal relative velocity of debris and carriers, leading to adhesion of debris g_a (Eq. 8) (dashed line) and minimal relative velocity of carriers g_c, leading to the detachment of debris of size r from their surface (Eq. 17) (solid line). The adhesion coefficient $\gamma = 0.74$ N/m, the radius of carriers $R = 6$ m. In the upper corner of the diagram all collisions between carriers lead to detachment of debris, while the lower corner corresponds to sticky collisions between carriers and debris.

to adhesion. Here a is the contact radius of the colliding particles, $R_{cd} = Rr/(R+r)$ – their effective radius.

The work, required to release a bound debris particle from a carrier surface, can be written in the form (Brilliantov et al., 2007; Brilliantov and Spahn, 2006):

$$W_a = \int_{a_0}^{a_{\text{sep}}} F_a \frac{d\xi}{da} da = q_0 \left(\pi^5 \gamma^5 D^2\right)^{1/3} (R_{cd})^{4/3} \quad, q_0 \simeq 1.457 \qquad (5)$$

Here the deformation ξ is related to the contact radius according to (Johnson et al., 1971):

$$\xi = \frac{a^2}{R_{cd}} - \sqrt{\frac{8\pi\gamma Da}{3}} \qquad (6)$$

The contact radius and the deformation in the equilibrium ($F_a(a_0) = 0$) can be written in the following way: $a_0 = (6\pi\gamma D R_{\text{eff}}^2)^{\frac{1}{3}}$, $\xi(a_0) = \frac{1}{3}(6\pi\gamma D)^{\frac{2}{3}} R_{\text{eff}}^{\frac{1}{3}}$. The contact radius of separation $a_{\text{sep}} = \left(\frac{3}{2}\pi\gamma D R^2\right)^{\frac{1}{3}}$ can be found from the condition: $dF_a/da = 0$. It corresponds to the minimal value of adhesive force (Eq. 4) or to maximal external pulling F_{sep}, which the adhesive interactions between carriers and debris can resist (Johnson et al., 1971):

$$F_{\text{sep}} = -F_a(a_{\text{sep}}) = \frac{3}{2}\pi\gamma R_{cd}. \qquad (7)$$

If the kinetic energy of colliding boulders and debris with effective mass $m_{cd} = m_c m_d/(m_c + m_d)$ (here m_c and m_c are respectively the mass of carrier and of a debris particle) in the final stage of the collision $W_{kin} = \frac{1}{2}m_{cd}V_{cd}^{\prime,2}$ is too small to overcome the adhesion barrier $W_a \geq W_{kin}$, then

$$V_{cd} < g_a = \sqrt{\frac{2W_a}{m_{cd}\varepsilon^2}} \sim r^{-5/6}, \qquad (8)$$

and the particles stick (Brilliantov and Spahn, 2006). The dependence of g_a on the radius of debris r is depicted on Fig. 2. The smaller the particles, the easier they stick to the surface of larger ones.

9

The amount of debris particles per unit volume, attaching to a carrier per unit time (debris adsorption rate) reads

$$I_-(r) = (R+r)^2 N_c(R) n_v(r) \int d\vec{V}_d d\vec{V}_c d\vec{e} f\left(\vec{V}_d\right) f\left(\vec{V}_c\right)$$
$$\times \left|\vec{V}_{cd} \cdot \vec{e}\right| \Theta\left(-\vec{V}_{cd} \cdot \vec{e}\right) \Theta\left(g_a - V_{cd}\right)$$

$$(9)$$

Here the Heaviside step-functions select particles which approach with the relative normal velocity, smaller than g_a.

Note that in Eq. (9) we do not account for effects induced by the flattening of the ring in the equatorial plane of the central planet. This implies the dependence of the particles density on the respective velocity dispersion. However, it will affect in the same manner the corresponding gain term I_+ (section 2.2). Because the steady state balance of free and adsorbed debris depends solely on the *ratio* of the kinetic coefficients I_- and I_+, the effect is expected to cancel out.

Performing the integration with the velocity distribution function (3), we obtain:

$$I_-(r) = A(r)n_v(r) \tag{10}$$

where

$$A(r) = \left(\frac{8\pi}{3}\right)^{1/2} N_c(R)(R+r)^2 \left(v_c^2 + v_d^2\right)^{1/2} \times$$
$$\left[1 - \left(1 + \frac{3W_a(r)}{\varepsilon^2 m_{cd}} \frac{1}{v_c^2 + v_d^2}\right) \exp\left(-\frac{3W_a(r)}{\varepsilon^2 m_{cd}} \frac{1}{v_c^2 + v_d^2}\right)\right] \tag{11}$$

Expanding the exponent for $r \ll R$ or $W_a \ll m_{cd}(v_c^2 + v_d^2)$, one gets the following expression for the kinetic coefficient A:

$$A(r) = 3\sqrt{6\pi} \frac{W_a^2(r)N_c R^2}{\varepsilon^4 m_d^2} \frac{1}{\left(v_c^2 + v_d^2\right)^{3/2}} \sim r^{-10/3} \tag{12}$$

10

2.2. Collisional production of debris

Let us consider a collision of two boulders, covered by small particles. Let $\vec{r}_1$ and $\vec{r}_2$ denote their positions and $\vec{V}_{c1}$, $\vec{V}_{c2}$ their velocities. The vector connecting their centres at the collision instant is $\vec{r}_{12} = \vec{r}_1 - \vec{r}_2 = r_{12} \cdot \vec{e}$, their relative velocity is $\vec{V}_{12} = \vec{V}_{c1} - \vec{V}_{c2}$, and the normal component of their relative velocity reads: $g = \left| \left(\vec{V}_{12} \cdot \vec{e} \right) \right|$. During the collision particles undergo the deformation $\xi = 2R - r_{12}$. For the purpose of calculation of debris production, we neglect the dissipative forces. Then the elastic force acting between the boulders during the collision obeys the Hertzian law:

$$F_H = \frac{\sqrt{R_{\text{eff}}}}{D} \xi^{3/2} \, . \tag{13}$$

Here $R_{\text{eff}} = R/2$ is the effective radius of the carriers. We also denote the effective mass of colliding carriers as $m_{\text{eff}} = m_c/2$. In the collision the maximal inertial force acting on debris particles sitting on the surface of carriers occurs in the moment, when the compression of the boulders is maximal:

$$F_{\text{in}} = \frac{1}{2} m_d \ddot{r}_{12} = \frac{1}{2} \frac{F_H \left(\xi_{\text{max}} \right)}{m_{\text{eff}}} m_d \, . \tag{14}$$

This maximal compression of boulders ξ_{max} is achieved, when the elastic energy $W_{\text{el}} = \int_0^{\xi_{\text{max}}} F_H d\xi$ equals the initial kinetic energy $\frac{1}{2} m_{\text{eff}} g^2$ of the normal component of the relative motion:

$$\xi_{\text{max}} = \left(\frac{5}{4} \frac{D m_{\text{eff}}}{R_{\text{eff}}^{1/2}} \right)^{2/5} g^{4/5} \tag{15}$$

We assume, that the debris particle leaves the surface of the carrier, if the projection of the maximal inertial force (Eq. 14) on the carrier's surface

11

normal (see Fig. 1) exceeds the maximal external pulling (Eq. 7), which the adhesive interactions between carriers and debris can resist:

$$F_{\text{in}} \cos\theta \geq F_{\text{sep}} \tag{16}$$

The debris can release from both boulders, from the side facing the collision partner. We ignore the process of immediate re-attachment of a debris particle on the collision partner. Small particles that are sitting on the contact surfaces of the colliding carriers are compressed during collision and do not release. However, the radius of a contact surface is much smaller, than radii of colliding icy boulders, therefore, this effect can be neglected. For simplicity we also neglect possible release of debris due to lateral motion of debris over the boulders' surface (rolling or sliding) induced by the action of inertial forces and shearing away of debris during grazing collisions of carriers.

Substituting Eqs. (13)-(15) in Eq. (16) and setting $\cos\theta = 1$, we obtain the minimal relative velocity of carriers, leading to the detachment of debris of size r from their surface:

$$g_c(r) = \frac{(324\pi)^{1/3}}{\sqrt{5}} \left(\gamma^{5/2} D\right)^{1/3} \left(\frac{\rho_c}{\rho_d^{5/2}}\right)^{1/3} \left(\frac{R_{\text{eff}}}{1 + \frac{r}{R}}\right)^{5/6} r^{-5/3} \tag{17}$$

The dependence of g_c on the radius of debris r is depicted in Fig. 2. For smaller particles a larger impact velocity is needed to release them in an impact. The total number of small debris particles produced in a collision of two carriers is

$$\Delta n_s(r) = 4\pi R^2 n_s(r) \int_0^{\pi/2} d\theta \sin\theta \, \Theta \left(F_{\text{in}} \cos\theta - F_{\text{sep}}\right) . \tag{18}$$

Evaluating the integral yields

$$\Delta n_s(r) = 4\pi R^2 n_s(r) \Theta(g - g_c) \times \left(1 - \left(\frac{g_c}{g}\right)^{6/5}\right) . \tag{19}$$

12

The total number density of debris particles of size r, released per unit time and unit volume in boulders collision, is given by:

$$I_+(r) = (2R)^2 N_c^2(R) \int d\vec{V}_{c1} \, d\vec{V}_{c2} \, d\vec{e} \, f\left(\vec{V}_{c1}\right) f\left(\vec{V}_{c2}\right)$$
$$\times \Theta\left(-\left(\vec{V}_{12} \cdot \vec{e}\right)\right) \left|\vec{V}_{12} \cdot \vec{e}\right| \Delta n_s(r). \tag{20}$$

Performing the integration, we obtain:

$$I_+ = B\left(N_d - n_v\right) \tag{21}$$

$$B = 16R^2 N_c \sqrt{\frac{\pi v_c^2}{3}} \left[\left(1 + \frac{5}{2}\alpha\right) \exp(-\alpha) - \frac{5}{2}\alpha^{\frac{3}{5}} \Gamma\left(\frac{7}{5}, \alpha\right)\right] \tag{22}$$

with the incomplete Gamma-function:

$$\Gamma(x, \alpha) = \int_\alpha^\infty dy \, y^{x-1} e^{-y}, \tag{23}$$

where

$$\alpha(r) = \frac{3g_c^2(r)}{4v_c^2} \sim r^{-10/3} \tag{24}$$

The expression (22) for B may be further simplified if we estimate the Gamma-function, using the steepest descend (Laplace) method, which yields:

$$B \simeq B_1 \exp(-\alpha), \tag{25}$$

where

$$B_1 = 16R^2 N_c \sqrt{\frac{\pi v_c^2}{3}} \frac{3}{5\alpha}, \qquad \text{if } \alpha \geq \frac{2}{5} \tag{26}$$

and

$$B_1 = 16R^2 N_c \sqrt{\frac{\pi v_c^2}{3}} \left[1 + \frac{5}{2}\alpha - \left(\frac{5}{2}\alpha\right)^{3/5} \left(\frac{29}{50} + \frac{\alpha}{10} - \frac{3}{4}\alpha^2\right)\right],$$
$$\text{if } \alpha \leq \frac{2}{5} \tag{27}$$

13
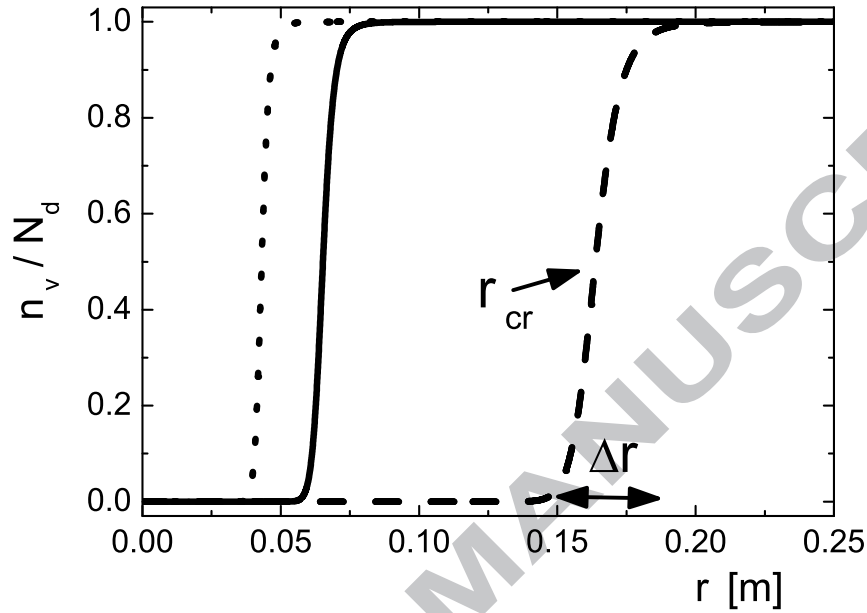
Figure 3: Dependence of the fraction of free debris n_v/N_d in the steady state on debris radius r for different values of velocity dispersion of carriers: $v_c = 0.001\,\mathrm{m/s}$ (dashed line), $0.005\,\mathrm{m/s}$ (solid line) and $0.01\,\mathrm{m/s}$ (dotted line). The velocity dispersion of debris is $v_d = 0.01\,\mathrm{m/s}$. The radius of boulders is taken as $R = 6\,\mathrm{m}$. Two regions are observed: if $r < r_{\mathrm{cr}}$, where r_{cr} is some critical radius, practically all debris are adsorbed, while all particles of radius $r > r_{\mathrm{cr}}$ are free. The critical radius of transition r_{cr} can be roughly determined as the point where $n_v/N_d = 1/2$. The transition between two regimes is very sharp, moreover, the width of the transition Δr decreases with the decreasing r_{cr}.

14
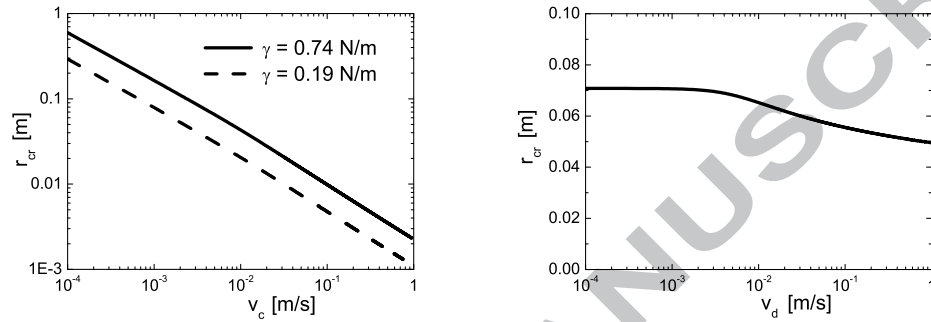
Figure 4: Dependence of the critical radius r_{cr} on velocity dispersion of carriers v_c for $v_d = 0.01\,\mathrm{m/s}$ (left panel) and on velocity dispersion of debris v_d for $v_c = 0.005\,\mathrm{m/s}$ (right panel). The critical radius r_{cr} does not change significantly even if v_d varies in the range of several orders, however, it sensitively depends on the velocity dispersion of carriers v_c. The radius of carriers $R = 6\,\mathrm{m}$. The adhesion coefficient $\gamma = 0.74\,\mathrm{N/m}$ (solid line) corresponds to theoretical value, calculated for a pure ice surface (Chokshi et al., 1993), $\gamma = 0.19\,\mathrm{N/m}$ (dashed line) was found in experiments of Gundlach et al. (2011).

15

3. Steady state abundance of small particles (debris)

The kinetic equation for the time evolution of the number density of free debris particles of size r reads:

$$\frac{dn_v(r,t)}{dt} = B(r)\left(N_d(r) - n_v(r,t)\right) - A(r)n_v(r,t) \qquad (28)$$

The solution of the equation has the form:

$$n_v(r,t) = n_v(r,\infty) + \left(n_v(r,0) - n_v(r,\infty)\right)\exp(-t/\tau), \qquad (29)$$

that is, $n_v(r)$ evolves exponentially to the steady-state value:

$$n_v(r,\infty) = \frac{N_d(r)}{1 + A\left(r\right)/B\left(r\right)} \qquad (30)$$

with the relaxation time:

$$\tau = 1/\left(A + B\right) \sim 1/N_c(R) \qquad (31)$$

The relaxation time is inversely proportional to $N_c(R)$, while the number density of free debris in the steady state $n_v(r,\infty)$ does not depend on the number density of carriers $N_c(R)$ (since both $A \sim N_c(R)$ and $B \sim N_c(R)$).

The fraction of free debris particles, calculated from Eq. (30) is shown in Fig. 3. Above a certain radius $r_{\mathrm{cr}} + \frac{1}{2}\Delta r$ all small particles remain free, while below $r_{\mathrm{cr}} - \frac{1}{2}\Delta r$ they are all attached to the surface of carriers. The transition between regimes of completely adsorbed and completely free debris is very sharp.

The critical radius of transition r_{cr} can be roughly determined as the point where $n_v/N_d = 1/2$ or $A\left(r_{\mathrm{cr}}\right) = B\left(r_{\mathrm{cr}}\right)$ in the following way:

$$r_{\mathrm{cr}} = \tilde{r}_{\mathrm{cr}}\left(\ln\frac{B_1(r_{\mathrm{cr}})}{A(r_{\mathrm{cr}})}\right)^{-3/10}, \qquad (32)$$

16

where

$$\tilde{r}_{\text{cr}} = \left(\frac{3}{5v_c^2}\right)^{3/10} \left(\frac{9\gamma R_{\text{eff}}}{4\rho_d}\right)^{1/2} \left(\frac{16\pi\rho_c D}{3}\right)^{1/5} \tag{33}$$

Taking into account the fact that the last factor in Eq. (32) only weakly depends on r_{cr}, we can approximate r_{cr} with a sufficient accuracy as

$$r_{\text{cr}} \simeq \tilde{r}_{\text{cr}} \left(\ln \frac{B_1(\tilde{r}_{cr})}{A(\tilde{r}_{cr})}\right)^{-3/10} \tag{34}$$

The transition becomes smoother with increasing r_{cr}. This is seen in Fig. 3 and may be easily shown analytically. Let us assume, that the fraction δ of debris of radius $r_{\text{cr}} - \frac{1}{2}\Delta r$, as well as the fraction $1 - \delta$ of debris of radius $r_{\text{cr}} + \frac{1}{2}\Delta r$, remains free, where δ is some small number. The transition width Δr has then the following form:

$$\Delta r \simeq \frac{3}{5} r_{\text{cr}} \frac{\ln\left(1/\delta - 1\right)}{\ln\left(B_1\left(r_{\text{cr}}\right)/A\left(r_{\text{cr}}\right)\right)} \tag{35}$$

Note, that if no fragmentation occurs in the system $(B\left(r\right) = 0)$, $n_v(r, \infty)$ becomes equal to zero: all debris will eventually stick to large particles even if $v_d >> g_a$. The critical radius r_{cr} tends to infinity in this case.

The magnitude of the critical radius r_{cr} is primarily governed by the inertial forces, acting on debris during collision of carriers and leading to the detachment of debris.

Therefore, according to Eqs. (32)-(33), the critical radius depends mostly on quantities, which are essential in the detachment processes (radii R and the velocity dispersion v_c of carriers) and has much weaker (logarithmic) dependence on quantities, assotiated with aggregation (the velocity dispersion v_d of debris). This statement is illustrated at Fig. 4. The larger the thermal velocity of colliding carriers, the smaller particles are released, therefore the

17

critical radius significantly decreases with increasing of v_c (left panel). In contrast, the dependence of r_{cr} on the debris velocity dispersion is very week: Fig. 4, right panel shows no significant variations of r_{cr}, when v_d varies over several orders of magnitude.

If the carriers become larger and more massive, their acceleration during the collision decreases and less debris leaves their surface. Therefore, the critical radius increases with increasing carrier size (Fig. 5, Eqs. (33)-(34)).

The value of adhesion coefficient $\gamma = 0.74\,\mathrm{N/m}$ was estimated theoretically for collisions of completely smooth particles (Chokshi et al., 1993). The adhesion coefficient of realistic ice particles can be few times smaller (Gundlach et al., 2011), which leads to a decreasing r_{cr}, due to reduction of the adhesion strength (see Figs. 4 and 5).

4. Application to planetary rings

Before we consider the application of our model to real systems it is worth to discuss some idealizations of the model and its impact on the adequate description of the planetary rings.

4.1. Justification of some model's idealizations

In the present study we propose the following simplified model: The system of interest is comprised of a population of large particles, the carriers of the same size, and smaller particles, debris, with some size distribution. Aggregation between carriers and debris is driven by surface adhesion. For given velocity dispersions of the two populations, their sizes, and material properties, we quantify the amount of the steady-state fraction of free debris particles, i.e. those not attached to the carrier particles. The balance depends

18
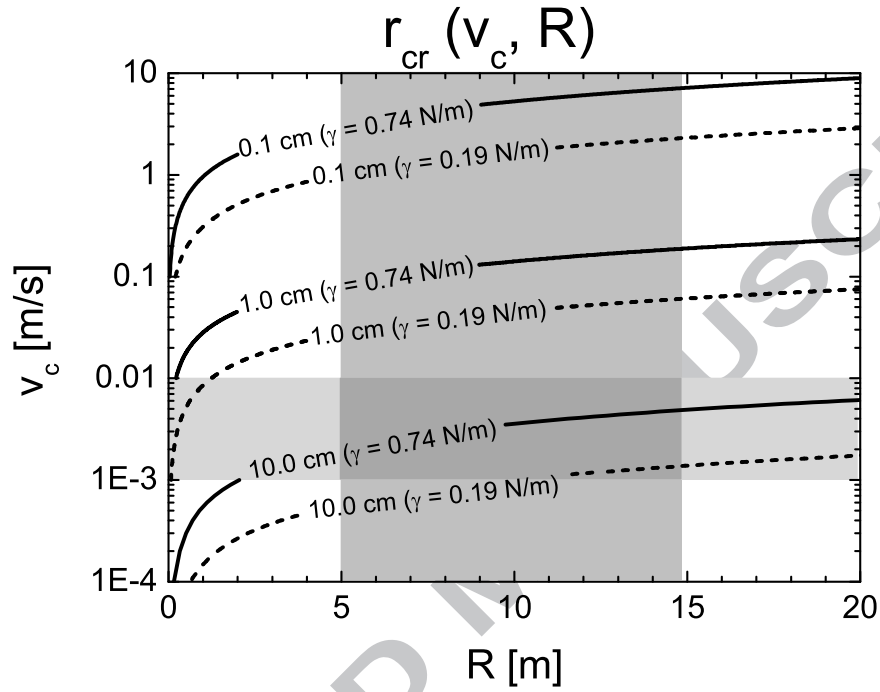
Figure 5: Contour graph, showing the dependence of the critical radius for debris release r_{cr} on velocity dispersion v_c and radii R of carriers. Solid contour lines are for the adhesion coefficient $\gamma = 0.74\,\mathrm{N/m}$ (Chokshi et al., 1993) and the dashed lines for $\gamma = 0.19\,\mathrm{N/m}$ (Gundlach et al., 2011). Parameter ranges plausible for Saturn's rings are highlighted in grey.

19
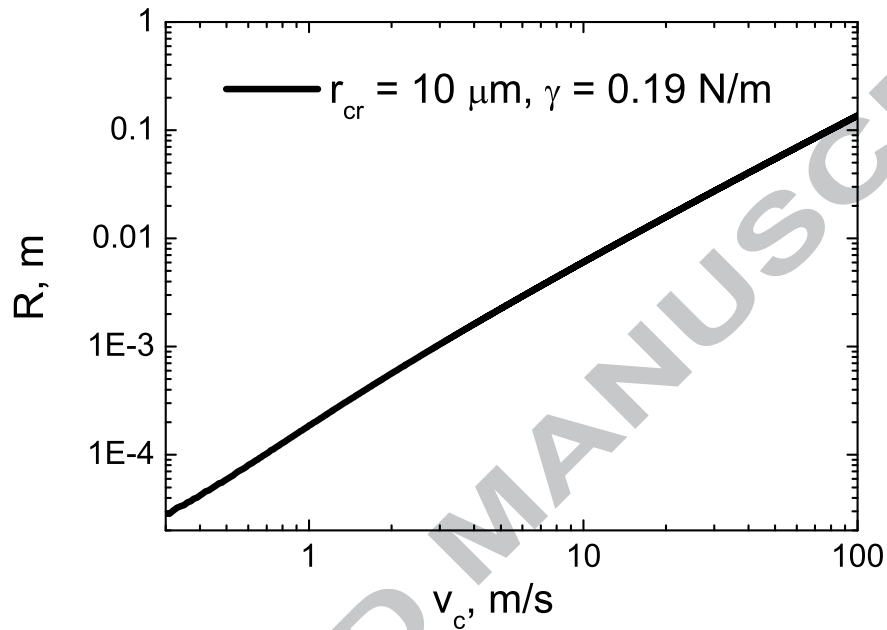
Figure 6: The case of micron sized dust: Carrier radius and velocity dispersion for fixed critical radius $r_{\mathrm{cr}} = 10\,\mu$m. The adhesion coefficient is $\gamma = 0.19\,$N/m (Gundlach et al., 2011). The abundant release of microscopic particles may be relevant in perturbed regions of the F ring. In this case fairly large collision velocities for the carriers are required and dominant carrier sizes not larger than few centimeters.

sensitively on the size of the debris particles. We obtain a critical radius, such that all smaller debris are practically absorbed by the carriers, while debris larger than the critical radius are all free.

In our model all debris particles are assumed to stick on the surfaces of carriers directly. There is no interaction between debris particles themselves, i.e. we neglect the process of particles attaching to debris that already sticks on a carrier, as well as the collisional aggregation of small particles. Effectively, these processes should tend to make the absorption of debris more efficient, since the relative strength of adhesion (compared to inertial forces) increases for smaller particles. Thus, qualitatively the inclusion of these processes should result in a somewhat larger critical radius than the one given directly by the model.

We also neglect the release of debris in collisions of carriers by lateral, shearing forces, and by the direct action of the carriers, shrugging off debris from their collision partner during a collision. These processes would make the collisional release more efficient and should work in the direction of a smaller value of the critical radius. One may expect that the two neglected effects compensate each other.

We can qualitatively estimate the influence of tangential motion of carriers in the following way. The maximal inertial force, acting on debris particles, can not exceed

$$F_{\text{in}} = \frac{1}{2}\frac{F_{\text{total}}\left(\xi_{\text{max}}\right)}{m_{\text{eff}}}m_d\,, \tag{36}$$

where the total force $F_{\text{total}} = \sqrt{F_H^2 + F_T^2}$ consists of Herzian force F_H and tangential force F_T. The tangential force $F_T \leq \mu F_H$, where μ is the friction coefficient. So if we take into account tangential interactions, the maximal

21

inertial force, acting on debris, will be only $\sqrt{1 + \mu^2}$ times larger. Taking into account that the friction coefficient of ice is estimated to be in the order of $\mu = 0.03$ according to the experimental data (Kietzig et al., 2010; Oksanen and Keinonen, 1982; Serway, 1995), it may be concluded that the effect of tangential interactions is negligible. One should note, however, that the friction coefficient of ice depends on temperature, velocity and normal load (Kietzig et al., 2010; Oksanen and Keinonen, 1982), and the effective friction coefficient of actual ring particles is unknown.

An impact of the rotational degrees of freedom may be also easily estimated. Indeed, the centrifugial force $F_{cen} = 2Rm_{\text{eff}}\omega^2$, where $\omega \approx g/2R$ is the characteristic rotational velocity of carriers, and g - their normal velocity, is significantly smaller than a typical Herzian force $\sqrt{R_{\text{eff}}}\xi^{3/2}/D$ for carriers of size up to 20 m. Therefore we do not take the centrifugial force into account in the present study.

Finally, we neglect any tidal forces and self-gravity in the system. Tidal forces should work against adhesion, leading to a lower critical radius, while self-gravity would enhance the tendency for clumping. Realistically, in Saturn's rings one expects the formation of self-gravity wakes (Salo, 1992a), i.e. clusters of ring particles, formed by gravitational instability, temporally bound but destroyed by shear when revolving under differential rotation around the planet. From the viewpoint of our model, one would expect the carrier particles to be arranged in such a wake pattern. In the wakes the population of debris particles, smaller than r_{cr}, should be absorbed on the carriers, while there still exists free debris in the rarefied regions between the wakes. The simplified kinetics of our model then describes average properties

22

of the rings, averaged over a spatial domain larger than the typical length scale of the wake pattern.

Note that we assume that only adhesive forces are responsible for the adsorption of small particles on the large ones, that is we, ignore gravitational forces. This is justified, since a simple analysis shows, that for the sizes of carriers (less than ~ 10 m) and debris (less than ~ 0.1 m) and for the values of adhesion coefficient, adopted in the present work, the gravitational forces indeed may be neglected, see also Fig.1 of Albers and Spahn (2006).

Strictly, our mathematical approach applies to a system with a bimodal size distribution. However, if we neglect any debris-debris interaction, the results can be interpreted for a system with a continuous size distribution of each of the sub-populations consisting of debris particles or carriers. On the one hand, if we vary the size of the debris particles, we observe a very abrupt transition from a state where practically all debris is attached to the carriers to a state where all debris is free (Fig. 3). This leads us to the definition of the critical radius, where we expect for a system with a distribution of debris particle sizes that all debris smaller than $r_{\rm cr}$ is absorbed. On the other hand, we observe a monotonic increase of the critical radius with increasing carrier size (Eqs. 33-34) so that for two carrier sizes $R^{(1)} < R^{(2)}$ in the system we expect $r_{\rm cr}^{(1)} < r_{\rm cr}^{(2)}$. Thus, in steady state all particles $r_{\rm cr}^{(1)} < r < r_{\rm cr}^{(2)}$, which cannot be absorbed by carriers of size $R^{(1)}$, will eventually be absorbed by the larger carriers of size $R^{(2)}$. Therefore, the effective critical radius for the total system is $r_{\rm cr}^{(2)}$. More generally, for a system with continuous distribution of carrier sizes we expect that the effective $r_{\rm cr}$ depends mostly on the largest carrier size $R_{\max}$ and we expect that the results presented in Fig. (3-5) hold,

23

if we replace R by $R_{\max}$. In this case, the velocity dispersion of the largest carriers is on the order of a few times $\Omega R_{\max}$ and the velocity dispersion of smaller carriers increases mildly with decreasing radius (Salo, 1992b). In such a way, the arguments developed in this paper for a bimodal system can be extended to the description of debris adsorption in systems with a continuous power-law size distribution $n(r) = n_0 r^{-\beta}$.

The maximal size of the main population of Saturn's ring particles is constrained to be on the order of $R_{\max} \approx 1 \dots 10\,\mathrm{m}$ (French and Nicholson, 2000; Zebker et al., 1985). The ring also contains a population of larger embedded moonlets, tens to hundreds of meters in size (Sremčević et al., 2007; Tiscareno et al., 2006; Tiscareno et al., 2008). However, these moonlets are rare and their distribution falls of much steeper towards larger sizes than for the population of main ring particles. Thus, for the moonlets the timescale to establish a collisional balance of debris absorption and release, Eq. 31) is huge and their effect on the amount of free debris particles can be neglected.

4.2. Absorption of dust in dense rings

Photometry of Saturn's A ring implies a very small fraction of free dust, if any. This conclusion seems to hold more generally for parts of the ring system with optical depth $\tau > 0.1$ but also for the dense rings of Uranus and Neptune (see discussion in Dones et al. (1993)). However, if not present in the system, dust should be rapidly replenished as the result of micrometeoroid bombardment on the rings (Cuzzi and Durisen, 1990; Durisen, 1984; Ip, 1983). One possibility is that non-gravitational forces rapidly remove dust from the system, such as electromagnetic and radiation forces (Burns et al., 1979; Burns et al., 1984; Rubincam, 2006; Vokrouhlický et al., 2007).

24

Although these forces can provide significant perturbations for micron sized particles, however, the unavoidable collisional interaction of the dust and macroscopic ring particles should enforce a locked dynamical evolution of both species and a preferential removal of dust by these processes appears unlikely. Alternatively, it has been suggested that sweep up of dust particles and their sticking on larger ring particles is responsible for the paucity of dust (Dones et al., 1993). This conclusion is supported by our results. In Fig. 6 we show the (maximal) carrier size R and velocity dispersions consistent with a micron sized critical radius r_{cr}. In fact, the release of micron sized dust from ring particles would require either implausibly large collision speeds or implausibly small radii of the carrier population. This large distance of the boundary for dust release from the domain of realistic ring parameters may explain why no free dust component is seen even in the highly perturbed regions of Saturn's main rings, such as the outer A ring beyond the Keeler gap, or the density waves at the strongest resonances in the rings (Dones et al., 1993).

The situation is different for the F ring of Saturn. Here, the confinement of the ring by Prometheus and Pandora, as well as the gravitational stirring of embedded moonlets and clumps (Cuzzi and Burns, 1988; Dermott, 1981; Kolvoord et al., 1990; Kolvoord and Burns, 1992; Lissauer and Peale, 1986; Showalter and Burns, 1982; Showalter et al., 1992; Winter et al., 2007) can lead to a fairly large velocity dispersion as high as several meters per second. The size of small particles in F ring is estimated to be in the order of several microns (Hedman et al., 2011), which corresponds according to our model to the dominant carrier size not exceeding few centimeters (Fig. 6). The

25

local or temporal perturbations may lead to detectable changes in the size distribution of the F ring dust (Hedman et al., 2010, 2011). Significant perturbations in the F ring, such as transitions of clumps of material through the core ring, are implied by Cassini data (Esposito et al., 2008; Charnoz, 2009), and they may occur even daily (Murray et al., 2008).

4.3. Lower size cut-off in Saturn's dense Rings

The lower size cut-off of the particles in Saturn's dense rings is to date probably best constrained (French and Nicholson, 2000) by a ring occultation of the star 28Sgr, observed from Earth (Nicholson et al., 2000), combined with Voyager photopolarimeter (PPS) stellar occultation data (Esposito et al., 1983). Assuming a power law size distribution, modelling of the scattered signal implies 1 cm as the lower size cut-off in the C ring and in the outer A ring, but 30 cm in the B ring and the inner to mid A ring (French and Nicholson, 2000). This is consistent within a factor of two with the analysis of radio occultations performed with the CASSINI Radio Science Subsystem (Marouf et al., 2008, see also Cuzzi et al. 2009), giving 5 mm in C and outer A, and 50 cm in the inner A ring.

If adhesion is the origin for the observed lack of small particles in the rings, then our expression for the critical radius should give a prediction for the lower size cut-off. In Fig. 5 we show the critical radius for various values of the velocity dispersion and (largest) size of carrier particles. The dependence on other parameters is weak, and the values used are given in the figure caption. From the identification of gravitational wakes in large parts of Saturn's rings (Colwell et al., 2006, 2007; French et al., 2007; Hedman et al.,

26

2007), it follows that the Toomre parameter for gravitational instability

$$Q = \frac{v_c \Omega}{3.36 G \Sigma} \tag{37}$$

should assume values around 2, or slightly smaller values. Here, Σ is the surface mass density of the rings, G is the gravitational constant, and Ω the Kepler frequency. This gives a rough constraint for the velocity dispersion of the carriers

$$v_c \approx 1.1 \times 10^{-3} \frac{m}{s} \left[\frac{Q}{2} \right] \left[\frac{\Sigma}{500 kg/m^2} \right] \left[\frac{2 \times 10^{-4} s^{-1}}{\Omega} \right] \tag{38}$$

On the other hand, dense, collision dominated rings should maintain a velocity dispersion on the order of Ω times particle diameter (Araki and Tremaine, 1986; Shukhman, 1984; Wisdom and Tremaine, 1988) so that

$$v_c \approx 4 \times 10^{-3} \frac{m}{s} \left[\frac{\Omega}{2 \times 10^{-4} s^{-1}} \right] \left[\frac{R}{10m} \right] \tag{39}$$

Shu et al. (1985) have estimated the collision velocity in the region of density waves, excited by of Mimas's 5:3 resonance in the A ring, as $0.4 - 3$cm/s.

In the figure we indicate plausible ranges for the velocity dispersion (0.1 cm/s to 1 cm/s) and largest particle sizes (5 m to 15 m, (French and Nicholson, 2000; Marouf et al., 2008; Tyler et al., 1983)) in grey. In this parameter range an adhesion coefficient of $\gamma = 0.74$ N/m gives critical radii from a few centimetres to a few tens of centimetres. This value of the adhesion coefficient follows from calculation of the strength of hydrogen bonding of clean ice surfaces in contact (Chokshi et al., 1993). For more realistic surfaces the effective γ might be lower. For comparison, we also show critical radii for $\gamma = 0.19$ N/m (Gundlach et al., 2011). In this case we obtain somewhat smaller values for r_{cr} around one to a few centimetres.

27

In conclusion, our results show that the observed lower size cut-off in Saturn's rings is consistent with the process of adhesional sticking of small particles on larger ring particles, taking into account a kinetic balance of sticking and release.

4.4. Increase of optical depth in perturbed regions

A local change of the steady state velocity dispersion of the ring matter can change the balance of adhesion and release of debris from the main ring particles. As a consequence, the input of energy and angular momentum in perturbed ring regions can lead to the collisional release of small debris particles, previously attached to larger ring particles, which could result in an observable increase of optical depth. This process was suggested as an explanation for the bright halos observed around the radial location of strong density waves in the A ring (Dones et al., 1993; Nicholson et al., 2008; Salo and Karjalainen, 2003). For example, the brightening measured in Dones et al. (1993) for the Mimas 5:3 resonance, was well fitted by Salo and Karjalainen (2003) with a photometric model. Salo and Karjalainen (2003) assumed the power-law size distribution with the slope $\beta = 3$ in the range from $r_{\mathrm{cr}} = 50\,\mathrm{cm}$ to $R_{\mathrm{max}} = 5\,\mathrm{m}$ in the background region, while the lower size cut-off was reduced to $r_{\mathrm{cr}} = 15\,\mathrm{cm}$ in the resonance zone due to release of small debris.

Another example are the propeller structures, forming as a response to the gravitational action of moonlets embedded in the rings (Spahn and Sremčević, 2000), which were observed in the A ring (Tiscareno et al., 2006). These structures appear brighter in the images, than the surrounding background, which indicates the increasing effective optical depth in the vicinity

28
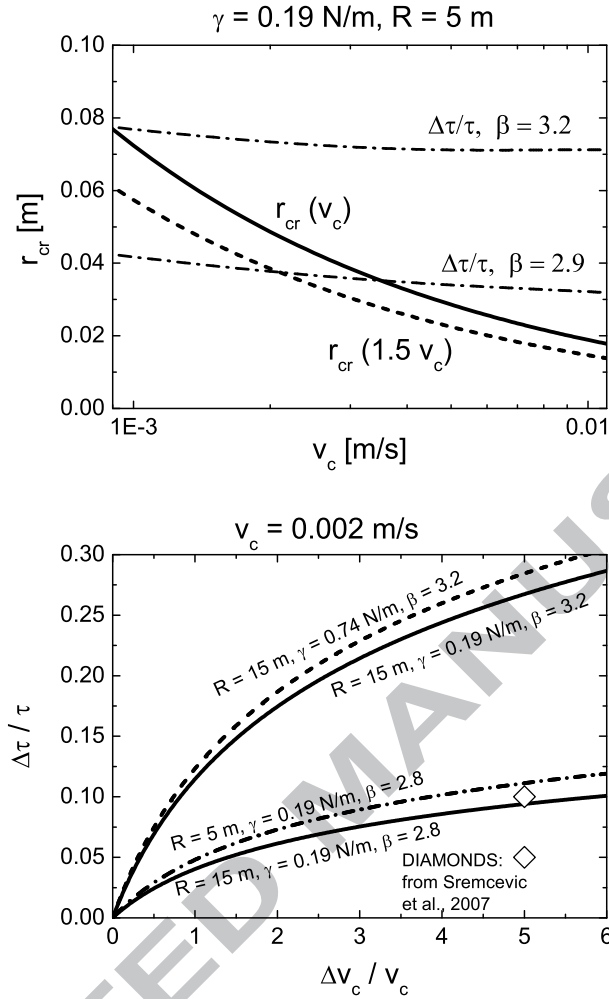
Figure 7: Upper panel: Critical radius $r_{\mathrm{cr}}(v_c)$ and r_{cr} for a 50% enhanced carrier velocity dispersion v_c. Also shown are the expected relative changes of optical depth (from equation 41) in the case of increasing of carrier velocity from v_c to $1.5v_c$, for two values of the size slope β. Lower panel: Relative change in optical depth depending on relative enhancement of v_c for fixed $v_c = 2\,\mathrm{mm/s}$. The size of the largest carrier R and the adhesion coefficient γ have a small influence on the optical depth variation. For comparison we also show symbols (diamonds) from dynamical and photometric simulations of a propeller structure (Salo and Schmidt, 2007) analyzed and compared to Cassini images by Sremčević et al. (2007) (see text for details).

29

of propellers (Tiscareno et al., 2008). Tiscareno et al. (2008, 2010) suggested, that this phenomena may be attributed to the disruption of the self-gravity wakes by the moonlet. In the present manuscript we consider another hypothesis, proposed by Sremčević et al. (2007), which assumes, that the additional material can be released in those regions where the perturbation of the moonlet induces collisions with a somewhat larger speed, when compared to the unperturbed ring.

An increase of the velocity of carriers by the factor of ten can decrease the critical radius by a factor of several (Eqs. (33)-(34)). If the critical radius decreases from $r_{cr,2}$ to $r_{cr,1}$ then material in the size range $r_{cr,1} < r < r_{cr,2}$ adds to the system the (dynamical) optical depth

$$\Delta\tau = \int_{r_{cr,1}}^{r_{cr,2}} \pi r^2 n\,(r)\,dr \tag{40}$$

if $n(r)$ is the size distribution of this material. If all ring material, including debris and carriers, follows the same size distribution in form of a power law $n(r) \sim r^{-\beta}$, then the relative enhancement of the optical depth can be expressed as

$$\frac{\Delta\tau}{\tau} = \frac{r_{cr,2}^{3-\beta} - r_{cr,1}^{3-\beta}}{R^{3-\beta} - r_{cr,1}^{3-\beta}} \tag{41}$$

where R is the size of the largest carrier and β the slope of the size distribution.

Examples for the so obtained estimate of the optical depth enhancements in perturbed ring regions are shown in fig. 7. One expects $\Delta\tau/\tau$ on the order of a few percent up to tens of a percent if the velocity dispersion is enhanced by a factor of five. For comparison we also show numbers derived from dynamical and photometric simulations of a propeller structure (Salo

30

and Schmidt, 2007) analyzed and compared to Cassini images by Sremčević et al. (2007). Here, debris particles were added to a ring background (dynamical optical depth $\tau = 0.5$, particle albedo $\varpi = 0.5$, steady state velocity dispersion $2 - 3\,\mathrm{mm/s}$, including self-gravity wakes) at those locations perturbed by an embedded moonlet where the perturbed impact velocity of ring particles exceeded $1\,\mathrm{cm/s}$. The debris followed Keplerian trajectories, with probabilities for re-absorption given by the particle positions obtained from the dynamical simulations. The radii of debris particles then were scaled, to adjust for the optical depth necessary to match the brightness of the propeller structure in images. Sremčević et al. (2007) obtained for the debris an optical depth of $\Delta\tau = 0.025$, using an albedo of $\varpi = 0.9$ for the debris particles. This value is shown in the lower panel of Fig. 7 as a diamond symbol. A roughly doubled optical depth of the debris is needed if debris particles have albedo $\varpi = 0.5$ (upper diamond symbol). We note that the debris optical depth from the simulations of Sremčević et al. (2007) represents an average over the whole simulations box. Locally, the optical depth enhancement is higher or lower. Also, the criterion for debris release $v_c > 1\,\mathrm{cm/s}$ does not strictly correspond to the perturbed velocity dispersion, which was used to derive the theoretical curves in Fig. 7. Nevertheless, the comparison demonstrates that the optical depth perturbations predicted by the theory developed in this paper are at least in reasonable agreement with available preliminary analysis of perturbed ring regions in Cassini data.

31

5. Conclusion and future work

We have presented a simple theoretical model to describe processes of adsorption and detachment of small debris particles on the surface of larger carrier particles. We have shown, that below a certain critical radius all debris particles are resting on the surface of the carriers. For parameters plausible for Saturn's rings, the value of this critical radius is consistent with an absence of subcentimeter particles in the dense rings. Particles with dimension greater than the critical radius may move freely in space. The critical radius decreases with decreasing effective adhesion coefficient, carrier size, and especially with increasing relative velocity of colliding boulders. In such a way, a perturbed velocity dispersion in the vicinity of moonlets or at the locations of satellite resonances in the rings may lead to the release of additional debris particles, enhancing the optical depth and affecting the brightness of satellite-generated structures in the images.

In future work we plan to improve the model of debris production, taking into account release of debris due to rolling (Dominik and Tielens, 1997), induced by the action of inertial forces.The theory could be extended by taking into account the dependence of velocity dispersion on the masses of particles. As for the comparison to data, it would be useful to evaluate the actual magnitude of the enhancement of velocity dispersions in perturbed regions of Saturn's rings. As a next step it would be worth to quantify the influence of released debris particles on the brightness of perturbed regions of the main rings and in certain regions of the F-ring.

Acknowledgements

References

Albers, N., Spahn, F., 2006. The influence of particle adhesion on the stability of agglomerates in Saturn's rings. Icarus 181, 292–301 .

Araki, S., Tremaine, S., 1986. The dynamics of dense particle disks. Icarus 65, 83–109.

Bridges, F.G., Hatzes, A., Lin, D.N.C., 1984. Structure, stability and evolution of Saturn's rings. Nature 309, 333–335.

Brilliantov, N., Bodrova, A., Krapivsky, P., 2009. A model of ballistic aggregation and fragmentation. J. Stat. Mech. , P06011.

Brilliantov, N.V., Albers, N., Spahn, F., Poeschel, T., 2007. Collision dynamics of granular particles with adhesion. Phys. Rev. E 76, 051302.

Brilliantov, N.V., Spahn, F., 2006. Dust coagulation in equilibrium molecular gas. Math. Comput. Simulat. 72, 93–97.

Brilliantov, N.V., Spahn, F., Hertzsch, J.M., Poeschel, T., 1996. Model for collisions in granular gases. Phys. Rev. E. 53, 5382–5392.

33

Burns, J.A., Lamy, P.L., Soter, S., 1979. Radiation forces on small particles in the solar system. Icarus 40, 1–48.

Burns, J.A., Showalter, M.R., Morfill, G.E., 1984. The ethereal rings of Jupiter and Saturn. In: Greenberg, R., Brahic, A. (Eds.), Planetary Rings. Tucson Arizona. University of Arizona Press. pp. 200–272.

Charnoz, S., 2009. Physical collisions of moonlets and clumps with the Saturn's F-ring core. Icarus 201, 191–197.

Chokshi, A., Tielens, A.G.G., Hollenbach, D., 1993. Dust coagulation. Astrophys. J. 407, 806–819.

Colwell, J.E., Esposito, L.W., Sremčević, M., 2006. Self-gravity wakes in Saturn's A ring measured by stellar occultations from Cassini. Geophys. Res. Lett. 33, L07201.

Colwell, J.E., Esposito, L.W., Sremčević, M., Stewart, G.R., McClintock, W.E., 2007. Self-gravity wakes and radial structure of Saturn's B ring. Icarus 190, 127–144.

Colwell, J.E., Nicholson, P.D., Tiscareno, M.S., Murray, C.D., French, R.G., Marouf, E.A., 2009. The Structure of Saturn's Rings. In: Dougherty, M. K., Esposito, L. W., Krimigis, S. M. (Eds.), Saturn from Cassini-Huygens. Springer. pp. 375–412.

Cuzzi, J., Burns, J.A., 1988. Charged particle depletion surrounding Saturn's F Ring. Icarus 74, 284–324.

34

Cuzzi, J., Clark, R., Filacchione, G., French, R., Johnson, R., Marouf, E., Spilker, L., 2009. Ring Particle Composition and Size Distribution. In: Dougherty, M. K., Esposito, L. W., Krimigis, S. M. (Eds.), Saturn from Cassini-Huygens. Springer. pp. 459–509.

Cuzzi, J.N., Durisen, R.H., 1990. Bombardment of planetary rings by meteoroids — General formulation and effects of Oort Cloud projectiles. Icarus 84, 467–501.

Davis, D.R., Weidenschilling, S.J., Chapman, C.R., Greenberg, R., 1984. Saturn ring particles as dynamic ephemeral bodies. Science 224, 744–747.

Dermott, S.F., 1981. The "braided" F-ring of Saturn. Nature 290, 454–457.

Dominik, C., Tielens, A.G.G.M., 1997. The physics of dust coagulation and the structure of dust aggregates in space. Astrophys. J. 480, 647–673.

Dones, L., Cuzzi, J., Showalter, M., 1993. Voyager photometry of Saturn's A ring. Icarus 105, 184–215.

Durisen, R.H., 1984. Particle erosion mechanisms and mass redistribution in Saturn's rings. Adv. Space Res. 4, 13–21.

Esposito, L., Meinke, B., Colwell, J., Nicholson, P., Hedman, M., 2008. Moonlets and clumps in Saturn's F ring. Icarus 194, 278–289.

Esposito, L.W., OCallaghan, M., Simmons, K.E., Hord, C.W., West, R.A., Lane, A.L., Pomphrey, R.B., Coffeen, D.L., Sato, M., 1983. Voyager photopolarimeter stellar occultation of Saturns rings. J. Geophys. Res. 88, 86438649.

35

French, R.G., Nicholson, P.D., 2000. Particle sizes inferred from stellar occultation data. Icarus 145, 502–523.

French, R.G., Salo, H., McGhee, C.A., Dones, L., 2007. HST observations of azimuthal asymmetry in Saturn's rings. Icarus 189, 493–522.

Goldreich, P., Tremaine, S., 1978. The velocity dispersion in Saturn's rings. Icarus 34, 227–239.

Gundlach, B., Kilias, S., Beitz, E., Blum, J., 2011. Micrometer-sized ice particles for planetary-science experiments. I. Preparation, critical rolling friction force, and specific surface energy. Icarus 214, 717723.

Hatzes, A.P., Bridges, F., Lin, D.N.C., Sachtjen, S., 1991. Coagulation of particles in Saturn's Rings: Measurements of the cohesive force of water frost. Icarus 89, 113–121.

Hedman, M.M., Nicholson, P.D., Salo, H., Wallis, B.D., Buratti, B.J., Baines, K.H., Brown, R.H., Clark, R.N., 2007. Self-Gravity Wake Structures in Saturn's A Ring Revealed by Cassini VIMS. Astron. J. 133, 2624–2629.

Hedman, M.M., Nicholson, P.D., Showalter, M.R., Brown, R.H., Buratti, B.J., Clark, R.N., Baines, K., Sotin, C., 2011. The Christiansen Effect in Saturns narrow dusty rings and the spectral identification of clumps in the F ring. Icarus, doi: 10.1016/j.icarus.2011.02.025 .

Hedman, M.M., Nicholson, P.D., Showalter, M.R., Cassini VIMS Team, 2010. Spectroscopic Identification of Clumps in the F Ring, in: AAS/Division for Planetary Sciences Meeting Abstracts, p. 987.

36

Ip, W.H., 1983. Collisional interactions of ring particles - The ballistic transport process. Icarus 54, 253–262.

Johnson, K., Kendall, K., Roberts, A., 1971. Surface energy and the contact of elastic solids. Proc. Roy. Soc. London A 324, 301–313.

Kietzig, A.M., Hatzikiriakos, S.G., Englezos, P., 2010. Physics of ice friction. J. Appl. Phys. 107, 081101.

Kolvoord, R.A., Burns, J.A., 1992. Three-dimensional perturbations of particles in a narrow planetary ring. Icarus 95, 253–264.

Kolvoord, R.A., Burns, J.A., Showalter, M.R., 1990. Periodic features in Saturn's F Ring: Evidence for nearby moonlets. Nature 345, 695–697.

Lissauer, J.J., Peale, S.J., 1986. The production of braids in Saturn's F Ring. Icarus 67, 358–374.

Longaretti, P.Y., 1989. Saturn's Main Ring Particle Size Distribution: An Analytic Approach. Icarus 81, 51–73.

Marouf, E., French, R., Rappaport, N., McGhee, C., Wong, K., Thomson, F., Anabtawi, A., 2008. Structure and physical properties of saturn's rings from cassini radio occultations. Abstracts for "Saturn after Cassini-Huygens" Symposium, Imperial College London, U.K., July 28 to August 1, p. 113.

Murray, C.D., Beurle, K., Cooper, N.J., Evans, M.W., Williams, G.A., Charnoz, S., 2008. The determination of the structure of Saturn's F ring by nearby moonlets. Nature 453, 739–744.

37

Nicholson, P., French, R., Tollestrup, E., Cuzzi, J., Harrington, J., Matthews, K., Perkovic, O., Stover, R., 2000. Saturns rings I: Optical depth profiles from the 28 Sgr Occultation. Icarus 145, 474–501.

Nicholson, P.D., Hedman, M.M., Clark, R.N., Showalter, M.R., Cruikshank, D. P., C.J.N., Filacchione, G., Capaccioni, F., Cerroni, P., Hansen, G.B., Sicardy, B., Drossart, P., Brown, R.H., Buratti, B.J., Baines, K.H., Coradini, A., 2008. A close look at saturns rings with cassini vims. Icarus 193, 182–212.

Ohtsuki, K., Emori, H., 2000. Local N-body simulations for the distribution and evolution of particle velocities in planetary rings. Astron. J. 119, 403–416.

Oksanen, P., Keinonen, J., 1982. The mechanism of friction of ice. Wear 78, 315–324.

Ramirez, R., Pöschel, T., Brilliantov, N.V., Schwager, T., 1999. Coefficient of restitution of colliding viscoelastic spheres. Phys. Rev. E 60, 4465–4472.

Rubincam, D.P., 2006. Saturn's rings, the Yarkovsky effects, and the Ring of Fire. Icarus 184, 532–542.

Salo, H., 1992a. Gravitational wakes in Saturn's rings. Nature 359, 619–621.

Salo, H., 1992b. Numerical simulations of dense collisional systems. II - Extended distribution of particle sizes. Icarus 96, 85–106.

Salo, H., Karjalainen, R., 2003. Photometric modeling of Saturns rings I.

Monte Carlo method and the effect of nonzero volume filling factor. Icarus 164, 428–460.

Salo, H.J., Schmidt, J., 2007. Release of impact-debris in perturbed ring regions: Dynamical and photometric simulations, in: AAS/Division for Planetary Sciences Meeting Abstracts #39, p. 425.

Schmidt, J., Ohtsuki, K., Rappaport, N., Salo, H., Spahn, F., 2009. Dynamics of Saturn's Dense Rings. In: Dougherty, M. K., Esposito, L. W., Krimigis, S. M. (Eds.), Saturn from Cassini-Huygens. Springer. pp. 413–458.

Serway, R., 1995. Physics for Scientists and Engineers, 4th edition. Harcorut Brace College Publishers, Orlando, FL.

Showalter, M., Pollack, J., Ockert, M., Doyle, L., Dalton, J., 1992. A photometric study of Saturn's F Ring. Icarus 100, 394–411.

Showalter, M.R., Burns, J.A., 1982. A numerical study of Saturn's F Ring. Icarus 52, 526–544.

Showalter, M.R., Nicholson, P.D., 1990. Saturn's rings through a microscope - Particle size constraints from the Voyager PPS scan. Icarus 87, 285–306.

Shu, F.H., Dones, L., Lissauer, J.J., Yuan, C., Cuzzi, J.N., 1985. Nonlinear spiral density waves: Viscous damping. Astrophys. J. 299, 542–573.

Shukhman, I., 1984. Collisional dynamics of particles in Saturn's rings. Sov. Astron. AJ 28, 574–585.

Spahn, F., Sremčević, M., 2000. Density patterns induced by small moonlets in Saturn's rings? Astron. Astrophys. 358, 368–372.

Sremčević, M., Schmidt, J., Salo, H., Seiß , Spahn, F., Albers, N., 2007. A belt of moonlets in Saturn's A ring. Nature 449, 1019–1021.

Tiscareno, M.S., Burns, J.A., Hedman, M.M., Porco, C.C., 2008. The Population of Propellers in Saturn's A Ring. Astron. J. 135, 1083–1091.

Tiscareno, M.S., Burns, J.A., Hedman, M.M., Porco, C.C., Weiss, J.W., Murray, C.D., Dones, L., 2006. Observation of "propellers" indicates 100-metre diameter moonlets reside in Saturn's A-ring. Nature 440, 648–650.

Tiscareno, M.S., Perrine, R., Richardson, D., Hedman, M.M., Weiss, J., Porco, C.C., Burns, J.A., 2010. An Analytic Parameterization Of Self-Gravity Wakes In Saturn's Rings, With Application To Occultations And Propellers. Astron. J. 139, 492503.

Tyler, G.L., Marouf, E.A., Simpson, R.A., Zebker, H.A., Eshleman, V.R., 1983. The microwave opacity of Saturn's rings at wavelengths of 3.6 and 13 cm from Voyager 1 radio occultation. Icarus 54, 160–188.

Vokrouhlický, D., Nesvorný, D., Dones, L., Bottke, W.F., 2007. Thermal forces on planetary ring particles: application to the main system of Saturn. Astron. Astrophys. 471, 717–730.

Weidenschilling, S.J., Chapman, C.R., Davis, D.R., Greenberg, R., 1984. Ring particles - Collisional interactions and physical nature, in: Planetary Rings, pp. 367–415.

Winter, O.C., Mourão, D.C., Giuliatti Winter, S.M., Spahn, F., da Cruz, C., 2007. Moonlets wandering on a leash-ring. Mon. Not. R. Astron. Soc. 380, L54–L57.

40

Wisdom, J., Tremaine, S., 1988. Local simulations of planetary rings. Astron. J. 95, 925–940.

Zebker, H.A., Marouf, E.A., Tyler, G.L., 1985. Saturn's Rings: Particle Size Distributions for Thin Layer Models. Icarus 64, 531–548.

- We describe adhesion and collisional release of debris in planetary rings.
- The maximal radius of adsorbed debris is found.
- The model explains the absence of subcentimeter particles in the rings.